C Journal of Carbon Research

MDPI

Review

Recent Progress in Synthesis and Application of Activated Carbon for CO_2 Capture

Chong Yang Chuah [1,2,*] and Afiq Mohd Laziz [1,2]

[1] Department of Chemical Engineering, Universiti Teknologi Petronas, Bandar Seri Iskandar 32610, Perak, Malaysia; afiq.laziz@utp.edu.my
[2] CO_2 Research Centre (CO2RES), Institute of Contaminant Management, Universiti Teknologi Petronas, Bandar Seri Iskandar 32610, Perak, Malaysia
* Correspondence: chongyang.chuah@utp.edu.my

Abstract: Greenhouse gas emissions to the atmosphere have been a long-standing issue that has existed since the Industrial Revolution. To date, carbon dioxide capture through the carbon capture, utilization, and storage approach has been one of the feasible options to combat the strong release of carbon dioxide into the atmosphere. This review focuses in general on the utilization of activated carbon as a tool when performing the carbon-capture process. Activated carbon possesses a lower isosteric heat of adsorption and a stronger tolerance to humidity as compared to zeolites and metal–organic frameworks, despite the overall gas-separation performance of activated carbon being comparatively lower. In addition, investigations of the activation methods of activated carbon are summarized in this review, together with an illustration of CO_2 adsorption performance, in the context of process simulations and pilot-plant studies. This is followed by providing future research directions in terms of the applicability of activated carbon in real CO_2 adsorption processes.

Keywords: greenhouse gas; activated carbon; CO_2 capture; adsorption

Citation: Chuah, C.Y.; Laziz, A.M. Recent Progress in Synthesis and Application of Activated Carbon for CO_2 Capture. *C* **2022**, *8*, 29. https://doi.org/10.3390/c8020029

Academic Editor: Patricia Luis

Received: 31 March 2022
Accepted: 6 May 2022
Published: 14 May 2022

1. Introduction

The emissions of greenhouse gases (GHGs) into the atmosphere have been a long-standing issue over the years that has existed since the onset of the Industrial Revolution in the 19th century. Carbon dioxide (CO_2), which is classified as one of the major components of GHGs, has experienced an increase in concentration throughout the entire timeframe, with CO_2 concentrations surpassing 400 ppm since 2013 [1–3]. This has resulted in undesirable consequences such as an increase in global temperatures, extreme weather events, and global warming. Nevertheless, considering the fact that the utilization of alternative renewable resources such as wind, tidal, and solar has been challenged by the difficulty to ensure a consistent supply of energy resources [4,5], it is expected that in the upcoming years, carbon-based fuels that are not limited to fossil fuels, coal, and natural gas, are foreseen to be the major sources of energy generation. Thus, as the combustion of fossil fuels has accounted for ca. 77% of the total contribution of CO_2 gas to the atmosphere [6], efforts to mitigate such undesirable releases should be the main focus of attention. This involves the use of carbon capture, utilization, and storage (CCUS) as an approach to capture CO_2 before its emission into the atmosphere [7,8].

In general, the total cost of the CCUS process is driven mainly by the CO_2 capture step, which accounts for approximately 70% of the overall system. Hence, it is highly desirable to select an appropriate method to capture CO_2 at the lowest possible cost. It has been observed that the utilization of scrubbing with the use of an alkanolamine-based solution is a reliable approach for CO_2 capture in pilot and industrial operations [9–11]. However, this unit operation has suffered from several shortcomings, namely a high energy penalty due to the presence of water, which possesses a large heat capacity in the amine solution and contributes to the corrosion of the vessel. As an illustration, the heat of sorption between

amine and CO_2 was reported to range from −50 to −100 kJ/mol at low CO_2 loading under ambient conditions [12,13].

In this regard, alternative unit operations have been proposed as a tool for CO_2 capture. This involves the use of solid porous adsorbents, which tend to demonstrate a much lower energy penalty as compared to amine absorption [14,15]. This is attributed to the fact that physical adsorption is the main mechanism of the CO_2 adsorption process. Furthermore, porous adsorbents are fully applicable in the variation in the operating conditions of the CO_2-containing feed gas stream; namely, postcombustion CO_2 capture, precombustion CO_2 capture, and the biogas upgrading process. In addition, several porous materials have been considered as potential candidates for effective CO_2 adsorption processes, and are not limited to zeolites, metal–organic frameworks (MOFs), and activated carbon. Nevertheless, zeolites, which tend to show a promising CO_2 separation performance, have been inhibited by the presence of moisture [16], which is typically present in CO_2-containing flue gas. MOFs, on the other hand, have demonstrated comparatively poorer hydrolytic and thermal stabilities as compared to zeolites and activated carbons [17]. Despite activated carbon generally showing a comparatively inferior CO_2 adsorption as compared to zeolites and MOFs (this shortcoming can be improved with additional modification, as elaborated in subsequent sections), its ease of regeneration after subsequent CO_2 adsorption (i.e., low isosteric heat of adsorption) and strong tolerance of the presence of moisture has ensured its practical feasibility [15].

Hence, in this review, recent advancements in the application of activated carbon in the field of the CO_2-capture process will be discussed. Since a substantial number of well-elaborated reviews [6,15,18,19] of the various activated methods to create high-porosity activated carbon have been published, in this investigation, a brief comparison will be provided to provide a quick overview of researchers that are still new in this field. In addition, recent advancements in the utilization of activated carbon in the CO_2-capture process will be elaborated to investigate CO_2-capture performance. Subsequently, the applicability of activated carbon in a realistic CO_2-capture process will be discussed by providing a brief description of the required performance evaluations, which are the swing adsorption process (temperature, pressure, or vacuum) and the breakthrough measurement. Furthermore, the application of activated carbon in a pilot-scale operation will be discussed in this review, followed by conclusions and ideas for future work to improve the overall feasibility of activated carbon in the industrial CO_2 adsorption process.

2. Activation Methods to Develop Activated Carbon for Effective CO_2 Capture

In general, activated carbon is described as amorphous stacks of carbon layers that are arranged with the aid of aliphatic bridging groups. Activated carbon can be obtained by utilizing various carbonaceous precursors, such as polymers, biomass, lignite, and coal, with the aid of pyrolysis. This is followed by the activation processes, which are generally classified into physical and chemical activation to allow the developed adsorbents to be capable of demonstrating effective CO_2 capture. A general comparison of these two approaches is summarized in Table 1.

Table 1. Comparison between physical and chemical activation for effective CO_2 adsorption of activated carbon [18,20,21].

Comparison	Physical Activation	Chemical Activation
General description	• Two-step process: (1) pyrolysis (carbonization); (2) physical activation at a higher temperature. • Creation of unsaturated surface (removal of oxygen-based functional groups to increase the basicity of carbon surface).	• Chemical activating agents are used to perform pyrolysis and activation simultaneously. • Addition of nitrogenous group can be performed at this stage to improve the overall basicity of activated carbon.

Table 1. *Cont.*

Comparison	Physical Activation	Chemical Activation
Operating conditions	• Pyrolysis (400–600 °C) at inert atmosphere • Physical activation (700–1000 °C) [a]	• Pyrolysis with chemical activation
Merits	• Environmentally friendly (without the use of chemicals).	• This method is commonly adopted as compared to physical activation. • Activation and pyrolysis can be performed simultaneously.
Limitations	• Physical activation can only be performed at a higher temperatures. • Two-step process (i.e., time-consuming). • Physical activation at >1000 °C is not effective due to a low degree of reactivity (with oxygen).	• Postsynthetic treatment (e.g., acid) is required to remove the residual reagents that are present on the activated carbon.
Possible reagents/mediums that can be adopted	• Inert gas (e.g., argon (Ar)) • Reactive gas (e.g., CO_2, hydrogen (H_2), oxygen, O_2) • Mixed gas (e.g., oxygen/nitrogen)	• Metal hydroxides (e.g., sodium hydroxide, potassium hydroxide) • Metal carbonates (e.g., sodium carbonate) • Acids (e.g., nitric acid, phosphoric acid) • Metal chlorides (e.g., zinc chloride, magnesium chloride) [b] • Nitrogen-containing medium (e.g., nitrogen gas, ammonia gas, amines) [c]

[a] Majority of the oxygen functionalities can be decomposed at 800–1000 °C. Strongly acidic functionalities (e.g., lactones, anhydrides, and carboxylic) and weakly acidic functionalities (e.g., phenol, carbonyl and quinone) can be decomposed at lower and higher temperatures, respectively; [b] After the pyrolysis process, metal chlorides will be converted to metal oxides and retained on the surface of the activated carbon; [c] This process typically requires the combination of another medium (e.g., metal hydroxides) to ensure a lower activation temperature, as compared to physical method.

3. Performance of Activated Carbon in CO_2 Capture

As summarized in Table 1, irrespective of the types of carbonaceous precursors used, the activation process is highly desirable to ensure that the developed porous materials are effective for CO_2 capture. Thus, in this section, reviews of the recent progress in the activation methods for effective CO_2 capture will be discussed, based on the activation method. Summary tables (Tables 2 and 3) that describe the overall CO_2 adsorption performance based on the variations in the activation process will be provided at the end of Sections 3.1 and 3.2, respectively, for effective comparison.

3.1. Physical Activation

Physical activation is a process where carbonaceous raw materials are activated via physical means through oxidizing agents such as air, CO_2, and steam. Nevertheless, prior to physical activation, the raw materials (i.e., precursors) are required to undergo pyrolysis or carbonization under inert conditions (e.g., Ar or N_2) [22]. This process creates a comparatively stable and heat-resistant compound for the development of activated carbon. In recent years, efforts to develop activated carbon through a single-activation step have been made due to the advantages of reduced operation, energy consumption and installation costs [23,24]. Furthermore, it has been reported that performing a single-step (rather than two-step) activation is feasible for obtaining activated carbon with improved characteristics, from the standpoint of creating activated carbons with higher surface area and porosity [23–25].

As elucidated above, three possible oxidizing agents have been used to create activated carbon. First, air is commonly adopted instead of pure nitrogen so as to remove the organic compounds and tar that are potentially generated during the carbonization process [23]. The presence of oxygen allows these carbons to be oxidized into CO_2 (Equation (1)), thus creating additional porosities on the generated activated carbon. Furthermore, additional tuning can be potentially conducted through the increase in oxygen purity by creating oxygen-enriched gas (OEG) instead of air to increase the oxidization capability of the carbonaceous materials [26]. Nevertheless, it should be noted that the oxygen content in the feed requires additional optimization as such increments generally resulted in a higher carbon oxidation, thus decreasing the overall yield of the activated carbon. The study of tuning the oxygen content in the feed during the physical activation process has been conducted by Plaza et al. [27]. In this investigation, three representative concentrations of oxygen (3%, 5% and 21%) were used to investigate the overall porosity of the activated carbon. It was observed that at the same activation temperature (500 °C), the overall yield of the activated carbon could be increased at lower oxygen content, due to a lower burn-off amount of external carbon. Furthermore, additional investigations into the change in the activation temperature elucidated the fact that a smaller micropore width could be introduced at a higher activation temperature due to the increase in the oxidation rate of the carbon conversion, which resulted in increased microporosity.

Additionally, CO_2 is also suitable for creating activated carbon. Under elevated temperatures (>700 °C), the utilization of CO_2 in the process allows Boudouard reaction (Equation (2)) to be thermodynamically favored. Therefore, the carbon structures can be removed to generate activated carbon with large surface areas [24,28,29]. In general, the activation temperature is highly critical due to Equation (2) being endothermic (+173 kJ mol^{-1}). Therefore, additional optimization of the activation temperature is required as it is expected that the diffusion of CO_2 into the carbonaceous materials is the rate limiting step. In a typical case, the selection of a suitable oxidization temperature can be performed by calculating the rate of mass loss at elevated temperature (i.e., 700 °C and higher) [28,30,31]. In addition, alteration to the holding temperature of the pyrolysis process is feasible to tune the performance. For instance, an increase in the holding time has resulted in a lower yield of activated carbon, due to the increase in the evaporation amount of the volatile matter, as elucidated by various authors [32,33]. Alternatively, the utilization of steam as the oxidizing agent is also feasible to create additional porosities on the activated carbon. This process can be performed by the introduction of hot steam, which is typically set at 700–800 °C. In this process, H_2O reacts with carbon to produce carbon monoxide (CO) and hydrogen (H_2), respectively, as indicated in Equation (3) (water–gas reaction) [34,35]. Nevertheless, from experimental studies, it is necessary to introduce an additional carrier gas (e.g., Ar or N_2) to transport the steam into the furnace for the oxidation process.

Based on the conditions as summarized in Table 2, irrespective of the type of the physical activation that will be adopted, the activation temperature is generally set between 700–900 °C to ensure effective pyrolysis, with the eventual aim of obtaining sufficient porosity for the CO_2 capture process. Nevertheless, it should be noted that substantial challenges have been encountered with the use of physical activation to produce the desired structure. For instance, physical activation lacks explicit tunability as compared to chemical activation in terms of adjustment of the pore size distribution and average pore size of the developed activated carbon [36,37]. Thus, most literature studies still adopt chemical activation despite physical activation generally being considered to be comparatively more environmentally friendly.

$$C + O_2 \rightleftharpoons CO_2 \quad (1)$$

$$C + CO_2 \rightleftharpoons 2CO \quad (2)$$

$$C + H_2O \rightleftharpoons CO + H_2 \quad (3)$$

Table 2. Performance of selected activated carbons that utilize physical activation for CO_2 capture.

Labels	Carbonaceous Feedstock	Activation Condition	Adsorption Condition	CO_2 Adsorption (mmol/g)	CO_2/N_2 Selectivity [a]	Ref.
A-3-650-83	Almond shells	3% O_2 (balance N_2), 650 °C, 83 min	25 °C, 1 bar	2.02	32	[27]
AC-700-800-1H	Date seeds	CO_2, 700 °C, 1 h	25 °C, 1 bar	2.88	-	[32]
AA750	Raw almond shells	CO_2, 700 °C	25 °C, 1 bar	2.50	-	[33]
AC-850-3	Pennsylvania anthracite	65.8% steam (balance N_2), 850 °C, 3 h	30 °C, 1 bar	2.64	-	[35]
ACS-1	Polyvinylidene chloride (PVDC)	N_2	0 °C, 1 bar	2.68	-	[22]
ACS-2	Polyvinylidene chloride (PVDC)	N_2	0 °C, 1 bar	2.75	-	[22]
ACS-3	Polyvinylidene chloride (PVDC)	N_2	0 °C, 1 bar	3.20	-	[22]
AOS-A900 (45%) [b]	Air-oxidized olive stones	CO_2, 900 °C	25 °C, 1 bar	2.52	-	[30]
AS	Almond shells	CO_2, 750 °C, 4 h	25 °C, 1 bar	2.70	20	[28]
B-800-15	Bamboo	CO_2, 800 °C, 15 min	25 °C, 1 bar	2.40	-	[29]
EC-RF	Resorcinol-formaldehyde aerogel	CO_2, 1000 °C, 3 h	25 °C, 20 bar	19.19	1.8	[31]
L-A850 (40%)—PEI [b]	Sewage sludge	Wet impregnation with PEI	25 °C, 1 bar	0.32	-	[30]
N-ACS	Poly(vinyl alcohol)	N_2 with water vapor, 800 °C, 1 h	25 °C, 1 bar	2.60	-	[38]
O-3-650-115	Olive stones	3% O_2 (balance N_2), 650 °C, 115 min	25 °C, 1 bar	2.11	30	[27]
OMCreo PAC 45% [b]	Ordered mesoporous silica templated with creosote	CO_2, 800 °C, 24 h	25 °C, 1 bar	2.18	-	[39]
OS	Olive stones	CO_2, 800 °C, 6 h	25 °C, 1 bar	3.00	18	[28]
PDS 800	Date seeds	CO_2, 800 °C, 1 h	25 °C, 1 bar	1.90	-	[32,40]
PR0	Hexamethylenetetramine and novolac-type phenolic resins	H_2O (steam), 830 °C, 1 h	25 °C, 1 bar	2.75	-	[41]
R-900-0.5h	Solid residues	CO_2, 900 °C, 30 min	25 °C, 1 bar	2.40	-	[38]
-	Peat (commercial activated carbon)	H_2O (steam)	25 °C, 1 bar	1.88	-	[42]

[a] Calculated using ideal adsorbed solution theory (IAST) unless otherwise stated; [b] The percentage refers to the burn-off degree (amount of carbon in the composite before and after the activation step).

3.2. Chemical Activation

In comparison, chemical activation is widely adopted to develop activated carbon with desired porosity. This involves the use of three broadly classified activators such as metal-based compounds (e.g., oxides, carbonates, hydroxides, and chlorides), acids and doping (e.g., heteroatoms such as nitrogen, amine-grafting and ionic liquids). These processes aim to attach additional functionalities or active sites that allow reversible interaction with CO_2. Thus, in this section, investigations on the methods adopted in the literature will be discussed to verify the merits and limitations of these two approaches.

3.2.1. Metal-Based Compounds

First, in the case of metal-based compounds, metal hydroxides are commonly utilized to generate porous activated carbon. Nevertheless, the activation mechanism of metal hydroxides has not been fully understood due to uncontrolled variables in both the reactivity of the carbonaceous precursors and experimental parameters [43]. Nevertheless, the widely accepted activation mechanism using metal hydroxides is illustrated through the following [44–48]: (a) redox reaction between various potassium compounds as the activating agent to etch the carbon framework (Equations (4)–(7)); (b) creation of H_2O and CO_2 molecules as the side reactions (Equations (8)–(10)) that can assist towards the further development of activated carbon via physical activation (Equation (3)); (c) intercalation of metallic carbon into the carbon lattices during the activation, which results in the expansion of the carbon lattice (Equation (4), (6) and (7)), as shown in Figure 1. After the activation completes, the residual K in the activated carbon can be removed by washing with the aid of an acidic solution. It is expected that the expanded carbon lattices are not usually feasible for return to their original non-porous structures after washing, thus generating activated carbon with high microporosity.

$$6MOH + 2C \rightleftharpoons 2M + 3H_2 + 2M_2CO_3 \quad (4)$$

$$CO_2 + C \rightleftharpoons 2CO \quad (5)$$

$$M_2CO_3 + 2C \rightleftharpoons 2M + 3CO \quad (6)$$

$$C + M_2O \rightleftharpoons 2M + CO \quad (7)$$

$$2MOH \rightleftharpoons M_2O + H_2O \quad (8)$$

$$CO + H_2O \rightleftharpoons CO_2 + H_2 \quad (9)$$

$$CO_2 + M_2O \rightleftharpoons M_2CO_3 \quad (10)$$

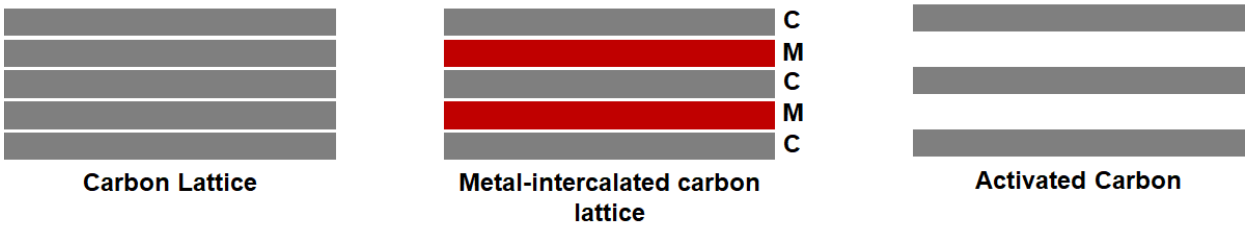

Figure 1. Potential activation mechanism for the creation of activated carbon by intercalation of metals into the carbon lattice (C).

Research efforts in improving the tunability of the micropore size of the activated carbon have been made with the use of different alkali metal ions as the activating agents. Thus, in the study conducted by Zhou et al. [49], the pore size of ultra-microporous carbon was examined using different alkali metal ions (Li^+, Na^+, K^+, Rb^+ and Cs^+), as shown in Figure 2a. Remarkably, based on the N_2 sorption isotherm and CO_2 adsorption isotherm (Figure 2b,c), the porosity of LiAC is much underdeveloped. As an illustration, changing the alkali metal ions from Li^+ to Cs^+ illustrates a sharp increment in BET (Brunauer–Emmett–Teller) surface area (111 to 1312 m^2/g) and total pore volume (0.07 to 0.70 cm^3/g), respectively. It was proposed that the activating strength of the metal ions was increasingly thermodynamically feasible (i.e., computed using change in Gibbs free energy, ΔG) when pyrolysis was performed. Based on the computed value of ΔG from Equation (12), the formation of LiAC and CsAC was reported to be 231 and −143 kJ/mol, respectively, indicating that the formation of LiAC is not spontaneous. Apart from this, all alkali metals except Li are feasible for use in generating metallic vapor (based on the boiling point) in a ready manner. This allows the metal ions to intercalate deeply into the carbon lattices, resulting in a well-developed porosity. Such a phenomenon is also supported

by Lee et al. [50], where the insertion of an alkali metal-graphite intercalation compound (AM-GIC) is feasible to obtain a relatively high BET surface area with the use of Cs as compared to other analogues (i.e., Li, Na, K and Rb), due to the possible extraordinary volume expansion for the as-developed activated carbon (Figure 2d).

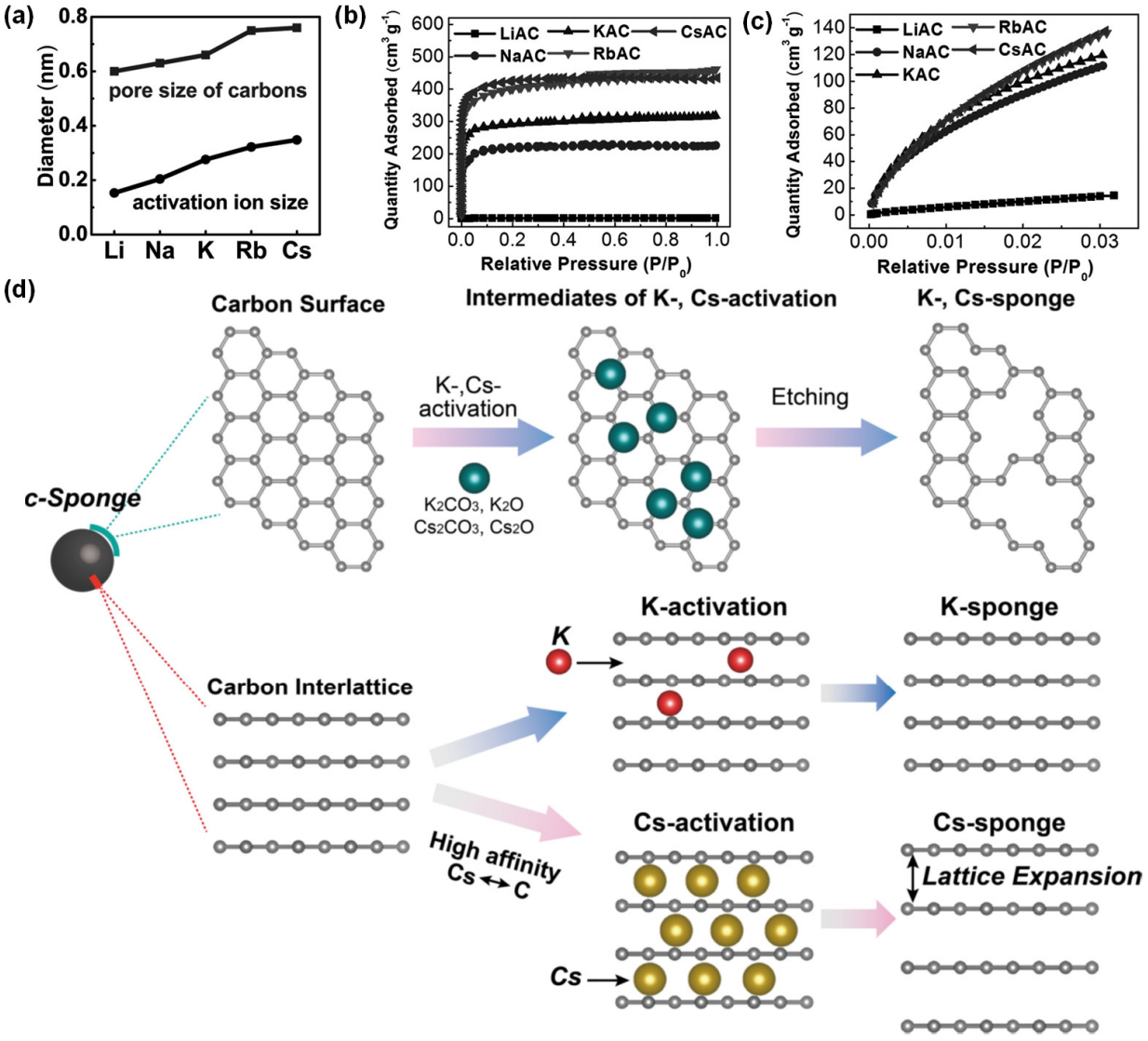

Figure 2. (**a**) Effect of the utilization of different sizes of the alkali metal ion on the average pore size of the developed activated carbon; (**b**) N_2 physisorption isotherm (77 K) and (**c**) CO_2 adsorption isotherm (273 K) of the activated carbon. Reprinted with permission from Ref. [49], Copyright 2016 Wiley-VCH Verlag GmbH & Co., Germany; (**d**) Proposed reaction mechanism between Cs-activation and K-activation. Reprinted with permission from Ref. [50], Copyright 2020 Wiley-VCH Verlag GmbH & Co., Germany.

As elucidated above, KOH is commonly adopted in activated carbon development due to the creation of an activated carbon that is highly microporous with a high specific surface area [51–53]. Nevertheless, due to its strong alkali nature, the removal of residual KOH after the synthesis has led to the creation of byproducts such as wastewater after the cleaning process [54]. Thus, several authors [54,55] have suggested using a K-based derivative such as potassium carbonate (K_2CO_3), which is the byproduct from the pyrolysis process when KOH is used as the activating agent (Equation (8)) instead. However, the reactivity of K_2CO_3 as the activating agent has been shown to differ greatly as compared to KOH. Based on thermal stability, K_2CO_3 melts at 891 °C and decomposes at 1200 °C, in

comparison to KOH (380 and 769 °C, respectively) [56]. Therefore, K_2CO_3 is comparatively less reactive due to its high thermal stability [57–59]. Furthermore, K_2CO_3 has been proven to be not thermodynamically favored with carbonaceous materials, based on the value of ΔG (>0) [60]. Thus, minimization of such undesirable behavior can been performed through a wet impregnation process to lower the decomposition temperature of K_2CO_3 (c.a. 890 °C), as reported by Hayashi et al. [58,59]. Nevertheless, based on the recent investigation performed by Kim et al. [56], the utilization of impregnated activated carbon with the use of K_2CO_3 possesses only ca. 70% of the BET surface area as compared to the use of KOH.

On the other hand, the utilization of metal chlorides has been considered as an approach for the creation of activated carbon. Zinc chloride ($ZnCl_2$), for instance, is commonly used due to its price competitiveness [61,62]. Efforts to understand the potential mechanism for the creation of activated carbon were made by Li et al. [63]. First, $ZnCl_2$ was also adopted, as compared to the aforementioned approaches (e.g., KOH), due to two possible reasons: (1) a low melting point (283–293 °C) that allows better contact with the carbon surface at the designated activated temperature; and (2) the creation of smaller micropores due to its small ionic radius (Zn^{2+}: 74 pm) as compared to K^+ (138 pm), which is a common reagent to create activated carbon. In general, $ZnCl_2$ will react with the residual water or hydroxyl functionalities that are present in the carbonaceous precursors to create zinc oxide (ZnO) and hydroxy dichlorozincic acid (H[$ZnCl_2$(OH)]) (Figure 3), which will remain in the pore structure. This framework is expected to retain the overall porosity once removed by acid washing, as shown in Figure 3. Nevertheless, based on the recent research conducted by Sarwar et al. [64], utilization of $ZnCl_2$ as the activation agent does not create a sufficiently high BET surface area as compared to the use of KOH or phosphoric acid.

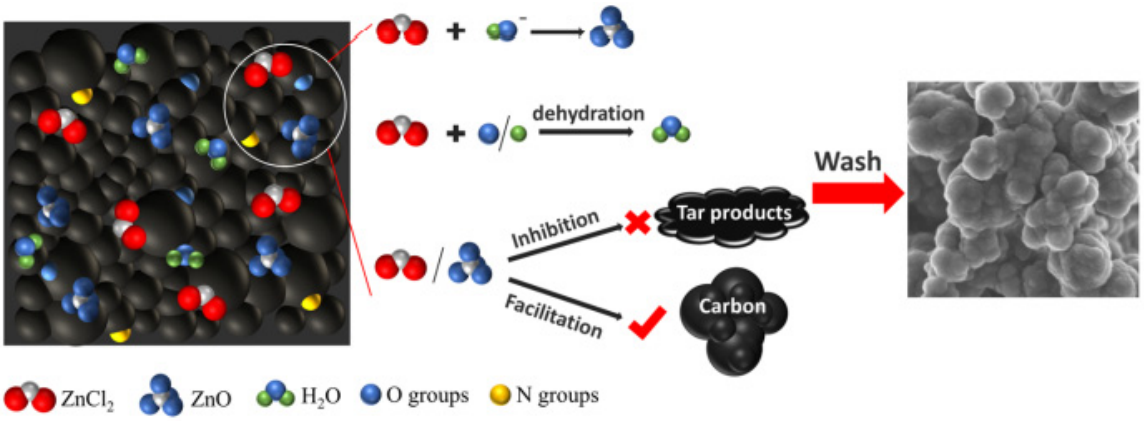

Figure 3. Proposed activation mechanism for the proposed formation of activated carbon with the aid of $ZnCl_2$. Reprinted with permission from Ref. [63] Creative Common License.

3.2.2. Acids

The utilization of alternative reagents such as phosphoric acid (H_3PO_4) has been potentially considered as compared to metal hydroxides or carbonates. This is attributed to its lower toxicological and environmental constraints with reference to $ZnCl_2$ (due to the potential release as chlorine (Cl_2) gas) as well as lower working temperature (as compared to KOH or NaOH). In general, H_3PO_4 has been proposed to be able to promote bond cleavage and/or crosslinked reactions on the carbon surfaces. Despite the actual mechanism of the function of H_3PO_4 as the activating agent remaining unclear, the proposed reactions can be simplified as shown in Equations (11) and (12), respectively, at mild activation temperatures (500–600 °C) [65–67]. Research has shown that the porous structures can be created on the activated carbon at high temperatures (>700 °C), however, inevitable pore collapse is expected to take place under such conditions [64,68]. Nevertheless, the creation of activated

carbon through this approach is not feasible for obtaining a reasonably high BET surface area, as compared to the use of KOH as the activating agent.

$$4H_3PO_4 \rightarrow P_4O_{10} + 6H_2O \quad (11)$$

$$P_4O_{10} + 10C \rightarrow P_4 + 10CO \quad (12)$$

3.2.3. Doping

Potential improvements in the CO_2 adsorption performance can be achieved through the modification of the surface chemistry that is present on carbonaceous materials. This can be performed through the addition of nitrogen-containing atoms or compounds into the carbonaceous precursors prior to the pyrolysis process, which are not limited to pyridinic-, amine/imine-, and pyrrolic-containing functional groups. This process, often termed as N-doping, is advantageous for CO_2 capture due to the introduction of nitrogen atoms making it feasible to improve the surface alkalinity via acid–base interaction, leading to an improved adsorption of acidic gases [69–71]. Apart from this, it is expected that the CO_2 adsorption capacity and selective adsorption of CO_2 with N-containing functionalities can be achieved through other methods such as hydrogen bonding or quadrupolar interaction, as in most cases the amine content in the activated carbon is fairly low (<4 wt%), based on the elemental analysis (EA) [72]. For instance, in the study by Yang et al. [36], a series of melamine-containing-functionalized phenolic resins as carbon precursors has been developed through the addition–condensation reaction with 2,4-dihydroxybenzoic acid (Ph), melamine (M) and formaldehyde, together with metal hydroxides (AOH) as the catalyst to create activated carbon (Figure 4a). Notably, despite with the addition of melamine which contains a substantially large number of N atoms, the nitrogen content that was present in the sample was low (<2 wt%), based on elemental analysis (EA) and X-ray photoelectron spectroscopy (XPS). This is possibly attributed to the addition of melamine into the framework which only served as the sacrificial template for the pyrolysis to create micropores of a larger pore size. Such a phenomenon is proven from the N_2 physisorption measurement (Figure 4b), where the addition of melamine (indicated as M) was used to increase the N_2 physisorption substantially, thus corresponding to an increase in BET surface area. In this regard, the amount of nitrogen content in the activated carbon can be potentially increased through the utilization of a nitrogen-rich carbon precursor, as performed by Sethia et al. [73]. It was observed that after the pyrolysis process, the resulting nitrogen content in the activated carbon remained high (c.a. 22.3 wt%), leading to a high CO_2 adsorption capacity (23.7 wt%) at ambient condition. Furthermore, the presence of large quantities of ultra-micropores that were less than 0.7 nm in diameter also served as an important role for effective CO_2 adsorption.

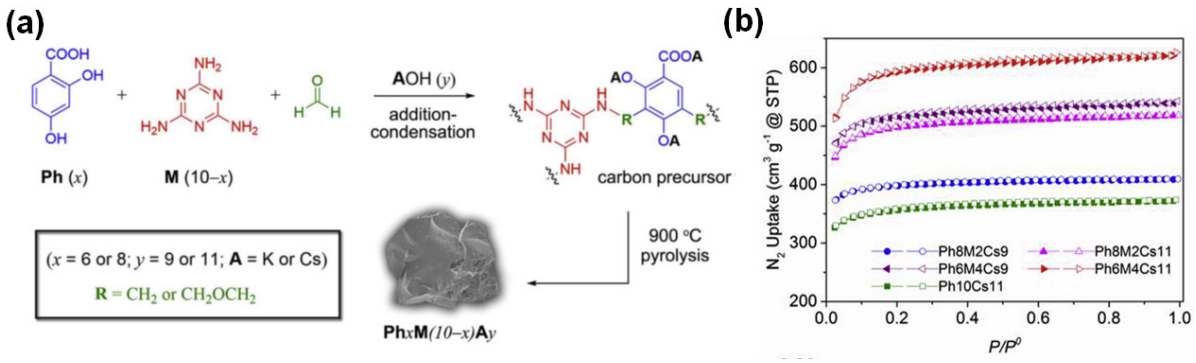

Figure 4. (**a**) Reaction scheme containing Ph, M formaldehyde; (**b**) N_2 physisorption isotherm of the developed activated carbon based on the reaction scheme in (**a**). Reprinted with permission from Ref. [36], Copyright 2019 Elsevier.

The addition of nitrogen-containing functionalities can be achieved through postsynthetic modification with amine-containing groups. Such an approach can be performed through the wet-impregnation process, which is analogous to the synthesis of amine-appended adsorbents (e.g., zeolites, mesoporous silicas, porous polymers, and metal-organic frameworks (MOFs)) [4,16,74,75]. In general, it is expected that with such incorporation it is feasible to increase the CO_2 adsorption at low partial pressure (<0.2 bar), which is critical in postcombustion CO_2 capture. Thus, in the study conducted by Plaza et al. [76], activated carbons are impregnated with different functional groups such as diethylenetriamine (DETA), polyethyleneimine (PEI) and pentaethylenehexamine (PEHA) for potential application in CO_2 capture. As expected, CO_2 adsorption is comparatively higher as compared to non-impregnated activated carbon, particularly for the case of PEHA-appended activated carbon, based on the pressure determined at < 0.005 bar. However, the incorporation of amine functionalities often has an undesirable effect on the actual practicability due to a large decrease in the accessible surface areas. As an illustration, a 90% decrease in the BET surface area has been observed when PEHA was attached to the activated carbon. This behavior is expected to influence the CO_2 adsorption kinetics substantially [71]. Furthermore, due to the expected chemisorption behavior between CO_2 and the amine groups, an extraordinarily high regeneration condition may be required to allow effective desorption of CO_2 from the synthesized adsorbents.

Apart from this, the utilization of nitrogen-containing functionalities can also be achieved with the use of reactive NH_3 gas. It is expected that at high temperature, the free radicals created from NH_3 may feasibly be decomposed into free radicals (i.e., NH_2, atomic hydrogen and NH) may react with the surface oxides that are present on the carbon surface to create nitrogen-rich functional groups. For instance, in the study conducted by Shafeeyan et al. [77], activated carbon was created through the flow of NH_3 gas with and without preoxidation (i.e., air of pure N_2). Based on the calculation of the BET surface area, the preoxidation process resulted in the partial blockage of micropores as well as the collapse of adjacent pore walls during the preoxidation stage [78], thus leading to a decrease in accessible surface area. This eventually resulted in a comparatively inferior CO_2 adsorption for the case of preoxidized activated carbon in comparison to heat-treated activated carbon.

Table 3. Performance of selected activated carbons that utilize chemical activation for CO_2 capture.

Labels	Carbonaceous Feedstock	Activation Condition [a]	Adsorption Condition	CO_2 Adsorption (mmol/g)	CO_2/N_2 Selectivity [b]	Ref.
a-CL	Celtuce Leaf	KOH, 800 °C, 1 h	25 °C, 1 bar	4.18	-	[51]
AC1	Bamboo chips	80% H_3PO_4, 500 °C, 4 h	25 °C, 50 bar	18.00	7.22 [c]	[67]
AC2	Rubber seed shell	Ionic liquid, 800 °C	25 °C, 1 bar	2.27	-	[79]
AC-2.5-600	Date seeds	KOH (2.5:1), 600 °C, 1 h	25 °C, 1 bar	2.18	-	[80]
AC-5	Rice husk	KOH (1:2), 600 °C, 1 h	25 °C, 1 bar	2.10	-	[69]
AC-850-3-NH_3-650	Pennsylvania anthracite	NH_3, 650 °C, 90 min	30 °C, 1 bar	2.55	-	[35]
AC-850-3-PEI	Pennsylvania anthracite	Wet impregnation with PEI	30 °C, 1 bar	0.21	-	[35]
AC-KOH	Corncob	KOH, 600 °C, 1 h	30 °C, 1 bar	3.39	-	[64]

Table 3. *Cont.*

Labels	Carbonaceous Feedstock	Activation Condition [a]	Adsorption Condition	CO_2 Adsorption (mmol/g)	CO_2/N_2 Selectivity [b]	Ref.
AC-PA	Corncob	H_3PO_4, 600 °C, 1 h	30 °C, 1 bar	2.25	-	[64]
AC-ZnCl	Corncob	$ZnCl_2$, 600 °C, 1 h	30 °C, 1 bar	2.84	-	[64]
AN800	Raw almond shells	NH_3, 800 °C, 2 h	25 °C, 1 bar	2.18	-	[33]
AOS-A900 (45%)–PEI	Air-oxidized olive stones	Wet impregnation with PEI	25 °C, 1 bar	1.98	-	[30]
AOS-NH_2	Air-oxidized olive stones	NH_3, 400 °C, 2 h	25 °C, 1 bar	2.25	-	[30]
AOS-NO400	Air-oxidized olive stones	8% NH_3 (balance air), 400 °C, 2 h	25 °C, 1 bar	2.11	-	[30]
CA-HC300	Glucose	KOH (1:2), 800 °C, 1.5 h	25 °C, 1 bar	4.30	-	[54]
CAC-5	Rice husk with chitosan	KOH (1:2), 600 °C, 1 h	25 °C, 1 bar	3.68	-	[69]
CeO_2/AC	Charcoal activated carbon	$Ce(NO_3)_2{\cdot}6H_2O$	25 °C, 1 bar	1.20	-	[81]
Coal-K-Im	Coal	KOH, 850 °C, 1 h	25 °C, 1 bar	5.88	-	[52]
CP-600	Trimethylsilyl imidazole, chloroacetonitrile	N_2, 600 °C, 2 h	25 °C, 1 bar	1.82	54	[73]
CsAC	2,4-dihydroxybenzoic acid (Ph), formaldehyde	CsOH, 900 °C, 2 h	25 °C, 20 bar	9.18	-	[49]
Cs-sponge-600	Marine sponge	CsOH, 600 °C, 1 h	25 °C, 1 bar	6.09	33 [c]	[50]
CuO(0.6)/AC	Commercial activated carbon	$Cu(NO_3)_2{\cdot}3H_2O$, 350 °C, 4 h	30 °C, 1 bar	2.20	60	[82]
H_2	Eucalyptus camaldulensis wood	H_3PO_4 (2:1), 450 °C, 1 h	30 °C, 1 bar	2.98	-	[20]
HK	Eucalyptus camaldulensis wood	KOH (3.5:1), 900 °C, 1 h	30 °C, 1 bar	4.10	-	[20]
HTA-400	Granular activated carbon (palm shell)	NH_3, 400 °C, 2 h	30 °C, 1 bar	1.41	-	[77]
HTA-800	Granular activated carbon (palm shell)	NH_3, 800 °C, 2 h	30 °C, 1 bar	1.64	-	[77]
KOH:FPV_850-1	Commercial activated carbon	KOH (1:1), 850 °C	25 °C, 35 bar	16.29	-	[55]
K-sponge-700	Marine sponge	KOH, 900 °C, 2 h	25 °C, 1 bar	4.82	9 [c]	[50]
L-A850 (40%)—PEI	Sewage sludge	Wet impregnation with PEI	25 °C, 1 bar	0.32	-	[30]

Table 3. *Cont.*

Labels	Carbonaceous Feedstock	Activation Condition [a]	Adsorption Condition	CO_2 Adsorption (mmol/g)	CO_2/N_2 Selectivity [b]	Ref.
MCa2FAL	African palm stones (lignocellulosic precursors)	H_3PO_4 + $CaCl_2$, 450 °C, 2 h	0 °C, 1 bar	7.20	-	[68]
MP48FAL	African palm stones (lignocellulosic precursors)	H_3PO_4, 600 °C, 2 h	0 °C, 1 bar	4.10	-	[68]
N-DETA	Commercial activated carbon (Norit CGP Super)	Wet impregnation with DETA (60 °C, 300 mbar, 30 min)	25 °C, 0.005 bar	0.27	-	[76]
N-PEHA	Commercial activated carbon (Norit CGP Super)	Wet impregnation with PEHA (60 °C, 300 mbar, 30 min)	25 °C, 0.005 bar	0.85	-	[76]
N-PEI	Commercial activated carbon (Norit CGP Super)	Wet impregnation with PEI (60 °C, 300 mbar, 30 min)	25 °C, 0.005 bar	0.36	-	[76]
NAC-1.5-600 [b]	Trimethylsilyl imidazole, chloroacetonitrile	KOH (1.5:1), 600 °C, 2 h	25 °C, 1 bar	5.39	62	[73]
OMCreo CA 4:1 850	Ordered mesoporous silica templated with creosote	KOH (4:1), 850 °C, 1 h	25 °C, 1 bar	4.19	-	[39]
OXA-400	Granular activated carbon (palm shell)	50% NH_3 (balance air), 400 °C, 2 h	30 °C, 1 bar	0.95	-	[77]
OXA-800	Granular activated carbon (palm shell)	50% NH_3 (balance air), 800 °C, 2 h	30 °C, 1 bar	1.48	-	[77]
PAC-2	Vitamin B9	KOH (2:1), 800 °C, 2 h	25 °C, 1 bar	3.66	-	[83]
PCSK-2-3-800	Poplar sawdust, sulfur containing waste liquid	$K_2C_2O_4$, 800 °C, 2 h	25 °C, 1 bar	3.80	-	[84]
Ph8M2Cs11	2,4-dihydroxybenzoic acid (Ph), melamine and formaldehyde	CsOH, 900 °C, 2 h	0 °C, 1 bar	3.64	-	[36]
Ph6M4K11	2,4-dihydroxybenzoic acid (Ph), melamine and formaldehyde	KOH, 900 °C, 2 h	0 °C, 1 bar	3.19	-	[36]
PR4-700	Hexamethylenetetr-amine and novolac-type phenolic resins	KOH (1:1), 700 °C, 1 h	25 °C, 1 bar	3.65	-	[41]

Table 3. *Cont.*

Labels	Carbonaceous Feedstock	Activation Condition [a]	Adsorption Condition	CO_2 Adsorption (mmol/g)	CO_2/N_2 Selectivity [b]	Ref.
SBL-MIP-800	Molecularly imprinted polymer with sugar beet leaves	KOH (2:1), 800 °C, 1 h	25 °C, 25 bar	17.90	13.7	[85]
VR5-1:1	Aliphatic vacuum residue with 5% mesophase content	KOH (1:1), 800 °C, 2 h	25 °C, 1 bar	3.63	-	[53]
VR5-4:1	Aliphatic vacuum residue with 5% mesophase content	KOH (4:1), 800 °C, 2 h	25 °C, 45 bar	34.09	-	[53]
$Z_{0.75}$	Eucalyptus camaldulensis wood	$ZnCl_2$ (0.75:1), 500 °C, 2 h	30 °C, 1 bar	1.90	-	[20]
-	Binary mixture of petroleum coke–palm kernel shell	K_2CO_3, 700 °C	25 °C, 1 bar	2.40	-	[42]
-	Olive waste	H_3PO_4 (1:1), 600 °C	25 °C, 18 bar	7.60	-	[66]
-	Petroleum coke	K_2CO_3, 700 °C	25 °C, 1 bar	2.26	-	[42]

NACS = nitrogen-modified resin-based activated carbon spheres [a] If the ratio is indicated in the table, it refers to the ratio between the chemical agent used with respect to the raw material; [b] The selectivities are calculated using ideal adsorbed solution theory (IAST), unless otherwise stated; [c] Henry's law is used to calculate the selectivity.

4. Evaluation of the Separation Performance of Activated Carbon in CO_2 Capture

In general, it is required to evaluate the performance of adsorbents in the field of CO_2 capture. Nevertheless, such evaluation has been often limited to the study of CO_2 adsorption at ambient condition (25 °C and 1 bar), which in most cases it is not relevant to the condition set for postcombustion CO_2 capture, as CO_2 partial pressure is typically less than 0.2 bar with N_2 as the major component. Thus, in this section, performance evaluation for CO_2 adsorption will be briefly discussed.

4.1. Equilibrium Gas Adsorption Isotherm

The single-component gas adsorption isotherm is expected to provide the most fundamental data in terms of the capability of the adsorbents in the field of CO_2 capture. Regardless of the available gas adsorption system, manometric (volumetric) or gravimetric method are typically used to perform the measurement (Figure 5a,b) [86,87]. The measurement of the pure component gas adsorption system relies on the assumption that competitive adsorption among different adsorbates can be ignored (CO_2 and N_2 in the case of postcombustion CO_2 capture). Furthermore, it is necessary to ensure that the measured gas adsorption fully equilibrates with the appropriate adjustment of the equilibration time. This is particularly evident if the adsorbents are postsynthetically modified with amine-appended frameworks due to the decreased accessibility of CO_2 gases onto the available active sites, considering the presence of dangling amine functionalities [71].

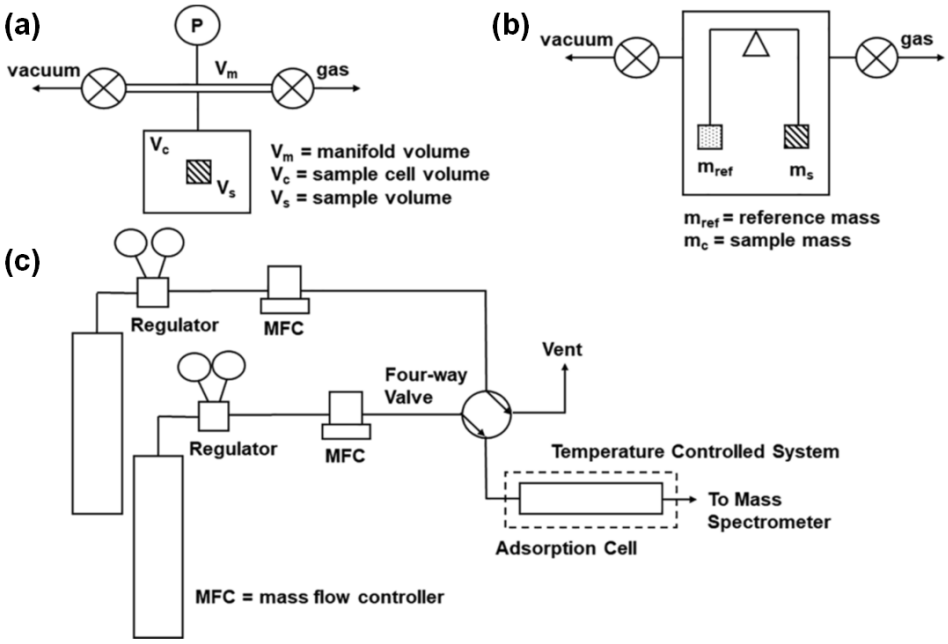

Figure 5. Measurement tools for effective investigation for CO_2-based separation process: (**a**,**b**) equilibrium measurement via volumetric and gravimetric method; (**c**) dynamic breakthrough measurement. Reprinted with permission from Ref. [87], Copyright 2019 Elsevier, Amsterdam, The Netherlands.

Hence, to allow a proper evaluation of the CO_2 separation performance of activated carbon, the mixed-gas selectivity of an adsorbent needs to be determined. From the perspective of CO_2/N_2 separation under postcombustion CO_2 capture, a typical composition of 5–20% CO_2 with the N_2 as the residual component is expected to be the most industrially relevant [17,88]. Thus, selectivity can be calculated by utilizing Equation (13), with S, p_i and q_i referring to the selectivity, partial pressure and quantity adsorbed of component i, respectively. A simplified manner to calculate the selectivity equation (i.e., ideal selectivity) involves the direct interpolation of CO_2 and N_2 adsorption at the specified partial pressure. For a more accurate prediction, calculating the mixed-gas selectivity is a common practice involving the utilization of a theoretical approach such as ideal adsorbed solution theory (IAST) [89,90]. This requires the solving of Equation (14) with the use of appropriate curve fitting for the gas adsorption isotherm. This involves the use of mole fraction of the bulk phase (known value, x_i and x_j) with the aim of calculating the mole fraction of the adsorbed phase (y_i and y_j). It should be noted that despite this calculation having been proven to be reliable, it is generally not feasible to perform accurate calculations on flexible frameworks such as MIL-53 and UTSA-300 which present breathing (gate-opening) effects upon CO_2 adsorption [13,87,91–93].

$$S = \frac{q_1/q_2}{p_1/p_2} \tag{13}$$

$$\int_0^{Py_i/x_i} \frac{q_i}{P} dP = \int_0^{Py_j/x_j} \frac{q_j}{P} dP \tag{14}$$

$$-Q_{st} = RT^2 \left(\frac{\partial \ln P}{\partial T} \right)_q \tag{15}$$

Next, the calculation of the isosteric heat of adsorption ($-Q_{st}$) that illustrates the binding energy of the active sites for CO_2 is important for separation performance as it evaluates the overall processing rate of the adsorbents [94]. It can be computed through Equation (15) (i.e., Clausius–Clapeyron Equation), which is a function of CO_2 loading (q). Thus, it is necessary to measure multiple gas adsorption isotherms over the desired temperature (T) range (usually at a span of 10 °C). However, due to the nature of the

expression, it is currently only feasible for isotherms that are fitted well with single- or dual-site Langmuir equations [2,95]. Thus, the Freundlich-based models which are used to express the explicit expression of pressure, P as a function of temperature, T are only feasible for modelling using the virial equation of state [96], despite the lack of clear physical meaning on the virial parameters presenting a major limitation on this approach. Alternatively, calorimetric measurement is expected to provide an accurate $-Q_{st}$ result, despite the experimental setting being quite challenging due to the need to ensure a well-controlled environment throughout the process.

4.2. Breakthrough Measurement

Multicomponent breakthrough analysis was considered as the common way to investigate the CO_2/N_2 separation performance of an adsorbent under dynamic operating conditions (Figure 5c). On the other hand, multicomponent equilibrium measurement remains challenging due to the necessity of sophisticated equipment and data analytics [88]. The major advantage of breakthrough analysis is the ability to cater for a simultaneous multicomponent feed stream towards the adsorption cell during the gas adsorption process in both dry and humid conditions. It should be noted that the accuracy of the breakthrough measurement is sensitive to the quantity of samples used [88]. Therefore, it is necessary to ensure that the sample quantity remains sufficient to provide meaningful results from the breakthrough curve.

4.3. Idealized Swing Adsorption

In a practical operating process for gas adsorption, pressure (PSA), temperature (TSA) or vacuum (VSA) swing adsorption are commonly involved. In the context of postcombustion-CO_2 capture, PSA is less practical considering the required energy penalty to pressurize the feed stream. Thus, TSA or VSA operation are expected to be the feasible approaches from the engineering design perspective. The investigation of the practical feasibility for the idealized swing adsorption process is performed by utilizing the pure component gas adsorption isotherm, as illustrated in Figure 6. This involves the parameter termed working capacity (WC), which is the amount of adsorbate that can be fully recovered after adsorption–desorption processes [97]. In the practical swing adsorption process, it is expected that the adsorption column will be fully saturated with CO_2 gas rather than the feed composition (i.e., CO_2/N_2 mixture). Thus, the evaluation for the swing adsorption process should be selected at the relevant desorption pressure by ensuring that the calculated WC is not overestimated [17].

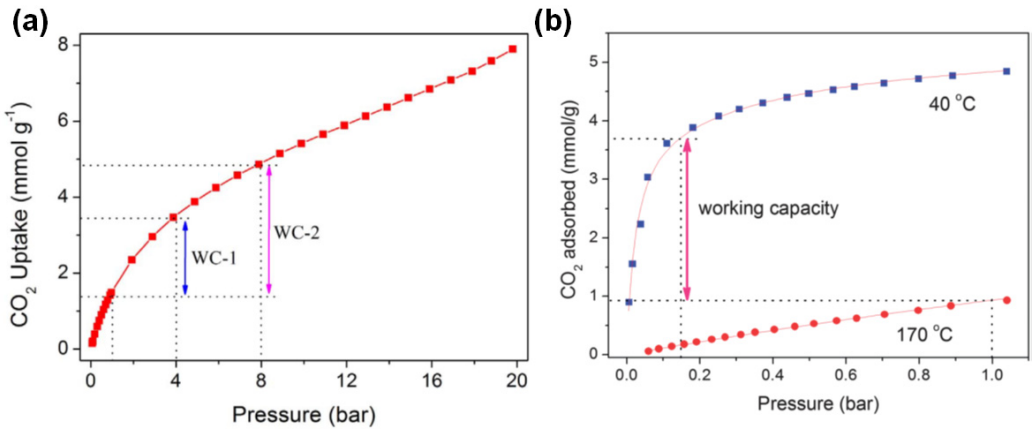

Figure 6. Illustration for the calculation of working capacity (WC) for idealized (**a**) PSA and (**b**) TSA. Reprinted with permission from Ref. [17], Copyright 2018 Elsevier and Ref. [98], Copyright 2013 Royal Society of Chemistry, London, United Kingdom.

5. Potential Utilization of Activated Carbon in Simulation and Pilot Scale Studies

Efforts to increase the practical feasibility of activated carbon in the field of CO_2 capture have been made to ensure that this unit operation can complement the current unit operations, namely cryogenic distillation and amine scrubbing that suffers a substantial energy penalty. Thus, efforts to utilize activated carbon for pilot scale studies have been performed through swing adsorption processes.

First, in the study conducted by Li et al. [99], a TSA system was integrated into a natural gas combined cycle (NGCC) and sequential supplementary firing combined cycle (SSFCC), where the process was performed with process simulation (Figure 7a). The adsorption/desorption system was developed in the form of a fluidized bed in comparison to a moving bed configuration as the latter suffers from poor regeneration due to limited heat transfer during desorption process [100]. This configuration allows the adsorbents to be circulated effectively in a closed-loop configuration. The adsorption/desorption system is maintained at a constant temperature by ensuring that the system is circulated with cooling water and thermal heat that is generated from the power plant, respectively. A cyclone, on the other hand is used to entrain the adsorber to allow CO_2-free flue gas to escape to the atmosphere through the stack. After the desorption process is performed, the desorbed CO_2 is utilized for applications such as enhanced oil recovery (EOR). Based on the calculated value of the regeneration heat (i.e., normalized based on per tonne of CO_2), it can be observed that the required energy for heat regeneration was comparatively high (Figure 7b) in comparison to amine-appended adsorbent polyethyleneimine (PEI) (impregnated with silica) and absorption monoethanolamine (MEA) due to activated carbon possessing a lower CO_2 adsorption capacity. Nevertheless, in terms of the power losses (which are caused by loss in power output and power auxiliaries as well as CO_2 compression during the operation), activated carbon consumed a much lower power due to a much lower isosteric heat of adsorption as compared to the amine-appended frameworks. This illustrates the potential benefits of activated carbon to be utilized in a TSA operating process.

Furthermore, the potential utilization of activated carbon has been investigated through the dual-reflux vacuum pressure swing adsorption (DR-VPSA) system [101,102]. This involves the use of a two-stage separation process by utilizing a single adsorption system that is partitioned into two sections. Such an approach performed as a single-stage adsorption system has been observed to be incapable of achieving appropriate CO_2 purity (i.e., >95%). The long-term stability of the adsorbents was examined by characterizing the performance of the adsorbents before (fresh) and after 808 h (used) continuous plant operation. Based on the available information, the total amount of accessible BET surface area decreased in the range of 18–30%, respectively, a loss that was attributed potentially to the presence of other undesirable substances such as dust, sulfur oxide (SO_x) and nitrogen oxide (NO_x). Such behavior was also reflected in the pure component gas adsorption (e.g., CO_2 and N_2) isotherm, which illustrated similar behavior. Thus, to improve the potential workability of the activated carbon, there is still some room for improvement in terms of the upstream treatment steps such as desulfurization, NO_x and SO_x removal, and dust filtering medium.

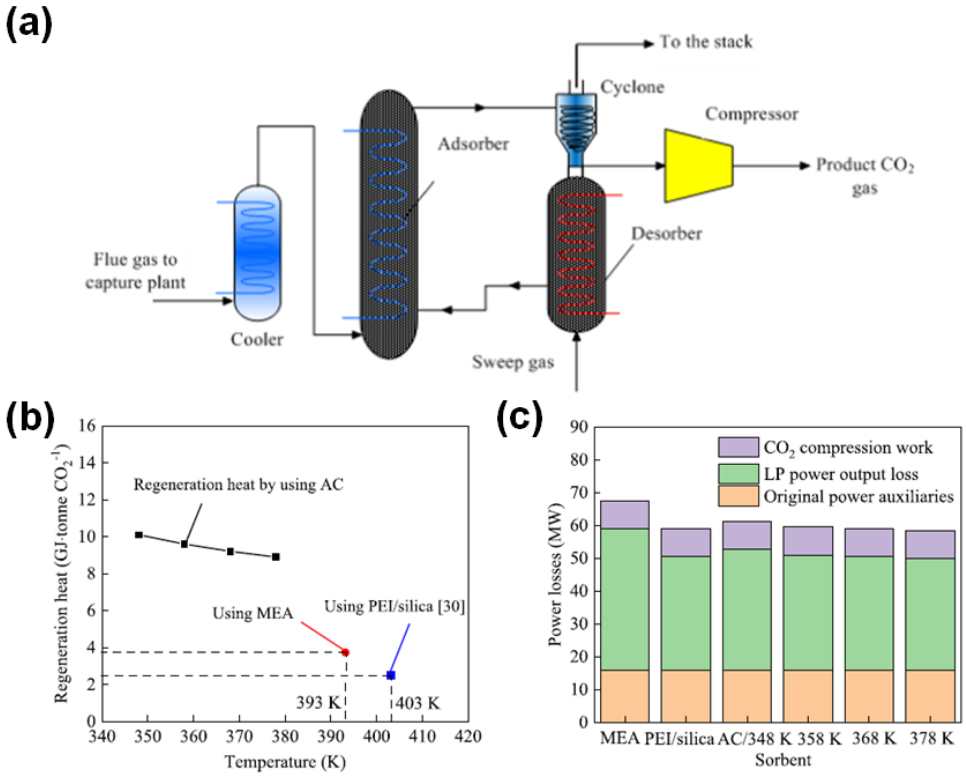

Figure 7. (**a**) Schematic illustration of adsorption system for TSA operation; (**b**) regeneration heat and (**c**) power loss for effective CO_2 capture, with the use activated carbon (AC), monoethanolamine (MEA) and amine-appended adsorbent (PEI/silica) as the medium. Reprinted with permission from Ref. [99] Creative Common License.

6. Conclusions and Future Perspective

In conclusion, activated carbon is capable of demonstrating effective CO_2 separation performance in comparison to other adsorbents such as zeolites and metal-organic frameworks, which tend to suffer poorer performance in humid conditions. Nevertheless, in terms of the controllability of the synthesis protocol, it is comparatively limited as the overall method is refined to two major approaches, namely physical and chemical modification. Thus, this has resulted in undesirable challenges for the effective tuning of the resulting properties, particularly of particle size which is less easily adjustable. Future efforts should therefore be conducted to allow the overall structure to be modified more easily, as compared to other porous materials.

Furthermore, it is also critical to emphasize the need to perform the experiments under more realistic conditions. For instance, as elaborated above, for the case of postcombustion-CO_2 capture, the presence of competitive adsorption among the various gases is expected to be prominent, leading to poor CO_2 adsorption performance. Such behavior is highly evident with the presence of undesirable impurities such as water and corrosive gases (e.g., SO_x, NO_x, etc.) that can potentially hamper the desired CO_2 adsorption during long-term operation. Therefore, the focus on gas adsorption should not only be restricted to pure component gas adsorption (which is an equilibrium measurement), but with more emphasis on the multicomponent gas adsorption process to increase the reliability of the studied adsorbents in practical operation.

Author Contributions: Conceptualization, C.Y.C.; writing—original draft preparation, C.Y.C. writing—review and editing, A.M.L. All authors have read and agreed to the published version of the manuscript.

Funding: The research was funded by Universiti Teknologi Petronas (UTP) Short Term Internal Research Funding (STIRF) with cost center: 015LA0-032.

Data Availability Statement: Not applicable.

Conflicts of Interest: The authors declare no conflict of interest.

References

1. Chuah, C.Y.; Lee, J.; Bao, Y.; Song, J.; Bae, T.-H. High-performance porous carbon-zeolite mixed-matrix membranes for CO_2/N_2 separation. *J. Membr. Sci.* **2021**, *622*, 119031. [CrossRef]
2. Lee, J.; Chuah, C.Y.; Tan, W.S.; Song, J.; Bae, T.-H. 3D-printed monolithic porous adsorbents from a solution-processible, hypercrosslinkable, functionalizable polymer. *Chem. Eng. J.* **2022**, *427*, 130883. [CrossRef]
3. Yang, Y.; Chuah, C.Y.; Bae, T.-H. Polyamine-Appended Porous Organic Copolymers with Controlled Structural Properties for Enhanced CO_2 Capture. *ACS Sustain. Chem. Eng.* **2021**, *9*, 2017–2026. [CrossRef]
4. Chuah, C.Y.; Li, W.; Samarasinghe, S.; Sethunga, G.; Bae, T.-H. Enhancing the CO_2 separation performance of polymer membranes via the incorporation of amine-functionalized HKUST-1 nanocrystals. *Micropor. Mesopor. Mater.* **2019**, *290*, 109680. [CrossRef]
5. Samarasinghe, S.; Chuah, C.Y.; Yang, Y.; Bae, T.-H. Tailoring CO_2/CH_4 separation properties of mixed-matrix membranes via combined use of two-and three-dimensional metal-organic frameworks. *J. Membr. Sci.* **2018**, *557*, 30–37. [CrossRef]
6. Sharma, A.; Jindal, J.; Mittal, A.; Kumari, K.; Maken, S.; Kumar, N. Carbon materials as CO_2 adsorbents: A review. *Environ. Chem. Lett.* **2021**, *19*, 875–910. [CrossRef]
7. Chuah, C.Y.; Kim, K.; Lee, J.; Koh, D.-Y.; Bae, T.-H. CO_2 absorption using membrane contactors: Recent progress and future perspective. *Ind. Eng. Chem. Res.* **2019**, *59*, 6773–6794. [CrossRef]
8. Chuah, C.Y.; Goh, K.; Yang, Y.; Gong, H.; Li, W.; Karahan, H.E.; Guiver, M.D.; Wang, R.; Bae, T.-H. Harnessing filler materials for enhancing biogas separation membranes. *Chem. Rev.* **2018**, *118*, 8655–8769. [CrossRef]
9. Fagerlund, J.; Zevenhoven, R.; Thomassen, J.; Tednes, M.; Abdollahi, F.; Thomas, L.; Nielsen, C.J.; Mikoviny, T.; Wisthaler, A.; Zhu, L. Performance of an amine-based CO_2 capture pilot plant at the Klemetsrud waste incinerator in Oslo, Norway. *Int. J. Greenh. Gas Control* **2021**, *106*, 103242. [CrossRef]
10. Natewong, P.; Prasongthum, N.; Reubroycharoen, P.; Idem, R. Evaluating the CO_2 capture performance using a BEA-AMP biblend amine solvent with novel high-performing absorber and desorber catalysts in a bench-scale CO_2 capture pilot plant. *Energy Fuels* **2019**, *33*, 3390–3402. [CrossRef]
11. Chahen, L.; Huard, T.; Cuccia, L.; Cuzuel, V.; Dugay, J.; Pichon, V.; Vial, J.; Gouedard, C.; Bonnard, L.; Cellier, N. Comprehensive monitoring of MEA degradation in a post-combustion CO_2 capture pilot plant with identification of novel degradation products in gaseous effluents. *Int. J. Greenh. Gas Control* **2016**, *51*, 305–316. [CrossRef]
12. Blanchon le Bouhelec, E.; Mougin, P.; Barreau, A.; Solimando, R. Rigorous modeling of the acid gas heat of absorption in alkanolamine solutions. *Energy Fuels* **2007**, *21*, 2044–2055. [CrossRef]
13. Sumida, K.; Rogow, D.L.; Mason, J.A.; McDonald, T.M.; Bloch, E.D.; Herm, Z.R.; Bae, T.-H.; Long, J.R. Carbon dioxide capture in metal–organic frameworks. *Chem. Rev.* **2012**, *112*, 724–781. [CrossRef]
14. Chuah, C.Y. *Microporous Materials with Tailored Structural Properties for Enhanced Gas Separation*; Nanyang Technological University: Singapore, 2019.
15. Creamer, A.E.; Gao, B. Carbon-based adsorbents for postcombustion CO_2 capture: A critical review. *Environ. Sci. Technol.* **2016**, *50*, 7276–7289. [CrossRef]
16. Chuah, C.Y.; Li, W.; Yang, Y.; Bae, T.-H. Evaluation of porous adsorbents for CO_2 capture under humid conditions: The importance of recyclability. *Chem. Eng. J. Adv.* **2020**, *3*, 100021. [CrossRef]
17. Yang, Y.; Chuah, C.Y.; Gong, H.; Bae, T.-H. Robust microporous organic copolymers containing triphenylamine for high pressure CO_2 capture application. *J. CO_2 Util.* **2017**, *19*, 214–220. [CrossRef]
18. Shafeeyan, M.S.; Daud, W.M.A.W.; Houshmand, A.; Shamiri, A. A review on surface modification of activated carbon for carbon dioxide adsorption. *J. Anal. Appl. Pyrolysis* **2010**, *89*, 143–151. [CrossRef]
19. González-García, P. Activated carbon from lignocellulosics precursors: A review of the synthesis methods, characterization techniques and applications. *Renew. Sustain. Energy Rev.* **2018**, *82*, 1393–1414. [CrossRef]
20. Heidari, A.; Younesi, H.; Rashidi, A.; Ghoreyshi, A. Adsorptive removal of CO_2 on highly microporous activated carbons prepared from Eucalyptus camaldulensis wood: Effect of chemical activation. *J. Taiwan Inst. Chem. Eng.* **2014**, *45*, 579–588. [CrossRef]
21. Caglayan, B.S.; Aksoylu, A.E. CO_2 adsorption on chemically modified activated carbon. *J. Hazard. Mater.* **2013**, *252*, 19–28. [CrossRef]
22. Carruthers, J.D.; Petruska, M.A.; Krishnan, G.; Hornbostel, M.; Bao, J. A New Activated Carbon for CO_2 Capture from Coal-Fired Boiler Flue Gas. *Adsorp. Sci. Technol.* **2013**, *31*, 185–197. [CrossRef]
23. Rodriguez-Reinoso, F.; Martin-Martinez, J.; Molina-Sabio, M.; Pérez-Lledó, I.; Prado-Burguete, C. A comparison of the porous texture of two CO_2 activated botanic materials. *Carbon* **1985**, *23*, 19–24. [CrossRef]
24. Savova, D.; Apak, E.; Ekinci, E.; Yardim, F.; Petrov, N.; Budinova, T.; Razvigorova, M.; Minkova, V. Biomass conversion to carbon adsorbents and gas. *Biomass Bioenergy* **2001**, *21*, 133–142. [CrossRef]
25. Linares-Solano, A.; De D. López-González, J.; Molina-Sabio, M.; Rodriguez-Reinoso, F. Active carbons from almond shells as adsorbents in gas and liquid phases. *J. Chem. Technol. Biotechnol.* **1980**, *30*, 65–72. [CrossRef]

26. Chuah, C.Y.; Anwar, S.N.B.M.; Weerachanchai, P.; Bae, T.-H.; Goh, K.; Wang, R. Scaling-up defect-free asymmetric hollow fiber membranes to produce oxygen-enriched gas for integration into municipal solid waste gasification process. *J. Membr. Sci.* **2021**, *640*, 119787. [CrossRef]
27. Plaza, M.; González, A.; Pis, J.; Rubiera, F.; Pevida, C. Production of microporous biochars by single-step oxidation: Effect of activation conditions on CO_2 capture. *Appl. Energy* **2014**, *114*, 551–562. [CrossRef]
28. González, A.; Plaza, M.; Rubiera, F.; Pevida, C. Sustainable biomass-based carbon adsorbents for post-combustion CO_2 capture. *Chem. Eng. J.* **2013**, *230*, 456–465. [CrossRef]
29. Khuong, D.A.; Nguyen, H.N.; Tsubota, T. Activated carbon produced from bamboo and solid residue by CO_2 activation utilized as CO_2 adsorbents. *Biomass Bioenergy* **2021**, *148*, 106039. [CrossRef]
30. Plaza, M.G.; Pevida, C.; Arias, B.; Casal, M.; Martín, C.; Fermoso, J.; Rubiera, F.; Pis, J. Different approaches for the development of low-cost CO_2 adsorbents. *J. Environ. Eng.* **2009**, *135*, 426–432. [CrossRef]
31. Far, H.M.; Lawson, S.; Al-Naddaf, Q.; Rezaei, F.; Sotiriou-Leventis, C.; Rownaghi, A.A. Advanced pore characterization and adsorption of light gases over aerogel-derived activated carbon. *Micropor. Mesopor. Mater.* **2021**, *313*, 110833. [CrossRef]
32. Ogungbenro, A.E.; Quang, D.V.; Al-Ali, K.A.; Vega, L.F.; Abu-Zahra, M.R. Physical synthesis and characterization of activated carbon from date seeds for CO_2 capture. *J. Environ. Chem. Eng.* **2018**, *6*, 4245–4252. [CrossRef]
33. Plaza, M.; Pevida, C.; Martín, C.F.; Fermoso, J.; Pis, J.; Rubiera, F. Developing almond shell-derived activated carbons as CO_2 adsorbents. *Sep. Purif. Technol.* **2010**, *71*, 102–106. [CrossRef]
34. Arena, U. Process and technological aspects of municipal solid waste gasification. A review. *Waste Manag.* **2012**, *32*, 625–639. [CrossRef] [PubMed]
35. Maroto-Valer, M.M.; Tang, Z.; Zhang, Y. CO_2 capture by activated and impregnated anthracites. *Fuel Process. Technol.* **2005**, *86*, 1487–1502. [CrossRef]
36. Yang, Y.; Goh, K.; Chuah, C.Y.; Karahan, H.E.; Birer, Ö.; Bae, T.-H. Sub-Ångström-level engineering of ultramicroporous carbons for enhanced sulfur hexafluoride capture. *Carbon* **2019**, *155*, 56–64. [CrossRef]
37. Zhang, J.; Gao, J.; Chen, Y.; Hao, X.; Jin, X. Characterization, preparation, and reaction mechanism of hemp stem based activated carbon. *Results Phys.* **2017**, *7*, 1628–1633. [CrossRef]
38. Zhang, C.; Wang, Y.; Zhang, X.; Wang, R.; Kou, L.; Wang, J.; Li, R.; Fan, C. Millimeter-level nitrogen modified activated carbon spheres assisted $Bi_4Ti_3O_{12}$ composites for bifunctional adsorption/photoreduction of CO_2. *Chem. Eng. J.* **2021**, *417*, 128218. [CrossRef]
39. García-Díez, E.; Castro-Muñiz, A.; Paredes, J.I.; Maroto-Valer, M.M.; Suárez-García, F.; García, S. CO_2 capture by novel hierarchical activated ordered micro-mesoporous carbons derived from low value coal tar products. *Micropor. Mesopor. Mater.* **2021**, *318*, 110986. [CrossRef]
40. Ogungbenro, A.E.; Quang, D.V.; Al-Ali, K.; Abu-Zahra, M.R. Activated carbon from date seeds for CO_2 capture applications. *Energy Procedia* **2017**, *114*, 2313–2321. [CrossRef]
41. Liu, J.; Sun, N.; Sun, C.; Liu, H.; Snape, C.; Li, K.; Wei, W.; Sun, Y. Spherical potassium intercalated activated carbon beads for pulverised fuel CO_2 post-combustion capture. *Carbon* **2015**, *94*, 243–255. [CrossRef]
42. Rashidi, N.A.; Yusup, S. Co-valorization of delayed petroleum coke–palm kernel shell for activated carbon production. *J. Hazard. Mater.* **2021**, *403*, 123876. [CrossRef] [PubMed]
43. Wang, J.; Kaskel, S. KOH activation of carbon-based materials for energy storage. *J. Mater. Chem.* **2012**, *22*, 23710–23725. [CrossRef]
44. Otowa, T.; Tanibata, R.; Itoh, M. Production and adsorption characteristics of MAXSORB: High-surface-area active carbon. *Gas Sep. Purif.* **1993**, *7*, 241–245. [CrossRef]
45. Lozano-Castello, D.; Calo, J.; Cazorla-Amoros, D.; Linares-Solano, A. Carbon activation with KOH as explored by temperature programmed techniques, and the effects of hydrogen. *Carbon* **2007**, *45*, 2529–2536. [CrossRef]
46. Raymundo-Pinero, E.; Azaïs, P.; Cacciaguerra, T.; Cazorla-Amorós, D.; Linares-Solano, A.; Béguin, F. KOH and NaOH activation mechanisms of multiwalled carbon nanotubes with different structural organisation. *Carbon* **2005**, *43*, 786–795. [CrossRef]
47. Qiao, W.; Yoon, S.-H.; Mochida, I. KOH activation of needle coke to develop activated carbons for high-performance EDLC. *Energy Fuels* **2006**, *20*, 1680–1684. [CrossRef]
48. Wang, H.; Gao, Q.; Hu, J. High hydrogen storage capacity of porous carbons prepared by using activated carbon. *J. Am. Chem. Soc.* **2009**, *131*, 7016–7022. [CrossRef]
49. Zhou, J.; Li, Z.; Xing, W.; Shen, H.; Bi, X.; Zhu, T.; Qiu, Z.; Zhuo, S. A new approach to tuning carbon ultramicropore size at sub-angstrom level for maximizing specific capacitance and CO_2 uptake. *Adv. Funct. Mater.* **2016**, *26*, 7955–7964. [CrossRef]
50. Lee, H.J.; Ko, D.; Kim, J.S.; Park, Y.; Hwang, I.; Yavuz, C.T.; Choi, J.W. Cesium Ion-Mediated Microporous Carbon for CO_2 Capture and Lithium-Ion Storage. *ChemNanoMat* **2021**, *7*, 150–157. [CrossRef]
51. Wang, R.; Wang, P.; Yan, X.; Lang, J.; Peng, C.; Xue, Q. Promising porous carbon derived from celtuce leaves with outstanding supercapacitance and CO_2 capture performance. *ACS Appl. Mater. Interfaces* **2012**, *4*, 5800–5806. [CrossRef]
52. Boujibar, O.; Ghamouss, F.; Ghosh, A.; Achak, O.; Chafik, T. Efficient CO_2 Capture by Ultra-high Microporous Activated Carbon Made from Natural Coal. *Chem. Eng. Technol.* **2021**, *44*, 148–155. [CrossRef]
53. Casco, M.E.; Martínez-Escandell, M.; Silvestre-Albero, J.; Rodríguez-Reinoso, F. Effect of the porous structure in carbon materials for CO_2 capture at atmospheric and high-pressure. *Carbon* **2014**, *67*, 230–235. [CrossRef]

54. Zhang, Z.; Luo, D.; Lui, G.; Li, G.; Jiang, G.; Cano, Z.P.; Deng, Y.-P.; Du, X.; Yin, S.; Chen, Y. In-situ ion-activated carbon nanospheres with tunable ultramicroporosity for superior CO_2 capture. *Carbon* **2019**, *143*, 531–541. [CrossRef]
55. Sreńscek-Nazzal, J.; Kiełbasa, K. Advances in modification of commercial activated carbon for enhancement of CO_2 capture. *Appl. Surf. Sci.* **2019**, *494*, 137–151. [CrossRef]
56. Kim, J.-H.; Lee, G.; Park, J.-E.; Kim, S.-H. Limitation of K_2CO_3 as a Chemical Agent for Upgrading Activated Carbon. *Processes* **2021**, *9*, 1000. [CrossRef]
57. Montes, V.; Hill, J.M. Activated carbon production: Recycling KOH to minimize waste. *Mat. Lett.* **2018**, *220*, 238–240. [CrossRef]
58. Hayashi, J.i.; Horikawa, T.; Takeda, I.; Muroyama, K.; Ani, F.N. Preparing activated carbon from various nutshells by chemical activation with K_2CO_3. *Carbon* **2002**, *40*, 2381–2386. [CrossRef]
59. Hayashi, J.i.; Horikawa, T.; Muroyama, K.; Gomes, V.G. Activated carbon from chickpea husk by chemical activation with K2CO3: Preparation and characterization. *Micropor. Mesopor. Mater.* **2002**, *55*, 63–68. [CrossRef]
60. Lu, C.; Xu, S.; Liu, C. The role of K_2CO_3 during the chemical activation of petroleum coke with KOH. *J. Anal. Appl. Pyrolysis* **2010**, *87*, 282–287. [CrossRef]
61. Chen, R.; Li, L.; Liu, Z.; Lu, M.; Wang, C.; Li, H.; Ma, W.; Wang, S. Preparation and characterization of activated carbons from tobacco stem by chemical activation. *J. Air Waste Manag. Assoc.* **2017**, *67*, 713–724. [CrossRef]
62. Liu, Z.; Huang, Y.; Zhao, G. Preparation and characterization of activated carbon fibers from liquefied wood by ZnCl2 activation. *BioResources* **2016**, *11*, 3178–3190. [CrossRef]
63. Li, B.; Hu, J.; Xiong, H.; Xiao, Y. Application and properties of microporous carbons activated by $ZnCl_2$: Adsorption behavior and activation mechanism. *ACS Omega* **2020**, *5*, 9398–9407. [CrossRef] [PubMed]
64. Sarwar, A.; Ali, M.; Khoja, A.H.; Nawar, A.; Waqas, A.; Liaquat, R.; Naqvi, S.R.; Asjid, M. Synthesis and characterization of biomass-derived surface-modified activated carbon for enhanced CO_2 adsorption. *J. CO_2 Util.* **2021**, *46*, 101476. [CrossRef]
65. Li, Y.; Zhang, X.; Yang, R.; Li, G.; Hu, C. The role of H_3PO_4 in the preparation of activated carbon from NaOH-treated rice husk residue. *RSC Adv.* **2015**, *5*, 32626–32636. [CrossRef]
66. Almoneef, M.; Jedli, H.; Mbarek, M. Experimental study of CO_2 adsorption using activated carbon. *Mater. Res. Express* **2021**, *8*, 065602. [CrossRef]
67. Wang, Y.; Liu, C.; Zhou, Y. Preparation and adsorption performances of mesopore-enriched bamboo activated carbon. *Front. Chem. Eng. China* **2008**, *2*, 473–477. [CrossRef]
68. Vargas, D.; Balsamo, M.; Giraldo, L.; Erto, A.; Lancia, A.; Moreno-Piraján, J. Equilibrium and dynamic CO_2 adsorption on activated carbon honeycomb monoliths. *Ind. Eng. Chem. Res.* **2016**, *55*, 7898–7905. [CrossRef]
69. He, S.; Chen, G.; Xiao, H.; Shi, G.; Ruan, C.; Ma, Y.; Dai, H.; Yuan, B.; Chen, X.; Yang, X. Facile preparation of N-doped activated carbon produced from rice husk for CO_2 capture. *J. Colloid. Interface Sci.* **2021**, *582*, 90–101. [CrossRef]
70. Lee, Y.; Chuah, C.Y.; Lee, J.; Bae, T.-H. Effective functionalization of porous polymer fillers to enhance CO_2/N_2 separation performance of mixed-matrix membranes. *J. Membr. Sci.* **2022**, *647*, 120309. [CrossRef]
71. Yang, Y.; Chuah, C.Y.; Bae, T.-H. Polyamine-appended porous organic polymers for efficient post-combustion CO_2 capture. *Chem. Eng. J.* **2019**, *358*, 1227–1234. [CrossRef]
72. Xing, W.; Liu, C.; Zhou, Z.; Zhang, L.; Zhou, J.; Zhuo, S.; Yan, Z.; Gao, H.; Wang, G.; Qiao, S.Z. Superior CO_2 uptake of N-doped activated carbon through hydrogen-bonding interaction. *Energy Environ. Sci.* **2012**, *5*, 7323–7327. [CrossRef]
73. Sethia, G.; Sayari, A. Comprehensive study of ultra-microporous nitrogen-doped activated carbon for CO_2 capture. *Carbon* **2015**, *93*, 68–80. [CrossRef]
74. Yang, Y.; Chuah, C.Y.; Bae, T.-H. Highly efficient carbon dioxide capture in diethylenetriamine-appended porous organic polymers: Investigation of structural variations of chloromethyl monomers. *J. Ind. Eng. Chem.* **2020**, *88*, 207–214. [CrossRef]
75. Nguyen, T.H.; Kim, S.; Yoon, M.; Bae, T.H. Hierarchical zeolites with amine-functionalized mesoporous domains for carbon dioxide capture. *ChemSusChem* **2016**, *9*, 455–461. [CrossRef] [PubMed]
76. Plaza, M.; Pevida, C.; Arenillas, A.; Rubiera, F.; Pis, J. CO_2 capture by adsorption with nitrogen enriched carbons. *Fuel* **2007**, *86*, 2204–2212. [CrossRef]
77. Shafeeyan, M.S.; Daud, W.M.A.W.; Houshmand, A.; Arami-Niya, A. Ammonia modification of activated carbon to enhance carbon dioxide adsorption: Effect of pre-oxidation. *Appl. Surf. Sci.* **2011**, *257*, 3936–3942. [CrossRef]
78. Pereira, M.F.R.; Soares, S.F.; Órfão, J.J.; Figueiredo, J.L. Adsorption of dyes on activated carbons: Influence of surface chemical groups. *Carbon* **2003**, *41*, 811–821. [CrossRef]
79. Mokti, N.; Borhan, A.; Zaine, S.N.A.; Zaid, H.F.M. Synthesis and Characterisation of Pyridinium-Based Ionic Liquid as Activating Agent in Rubber Seed Shell Activated Carbon Production for CO_2 Capture. *J. Adv. Res. Fluid Mech. Therm. Sci.* **2021**, *82*, 85–95. [CrossRef]
80. Abuelnoor, N.; AlHajaj, A.; Khaleel, M.; Vega, L.F.; Abu Zahra, M. Single Step Synthesis and Characterization of Activated Carbon from Date Seeds for CO_2 Capture. In Proceedings of the 15th International Conference on Greenhouse Gas Control Technologies, Abu Dhabi, United Arab Emirates, 15–18 March 2021.
81. Lahuri, A.H.; Ling, M.N.K.; Rahim, A.A.; Nordin, N. Adsorption kinetics for CO_2 capture using cerium oxide impregnated on activated carbon. *Acta Chim. Slov.* **2020**, *67*, 570–580. [CrossRef]
82. Chen, G.; Wang, F.; Wang, S.; Ji, C.; Wang, W.; Dong, J.; Gao, F. Facile fabrication of copper oxide modified activated carbon composite for efficient CO_2 adsorption. *Korean J. Chem. Eng.* **2021**, *38*, 46–54. [CrossRef]

83. Wang, X.; Hui, W.; Hu, A.; Li, X.; Li, Y.; Wang, H. A synthesis of porous activated carbon materials derived from vitamin B9 base for CO_2 capture and conversion. *Mater. Today Chem.* **2021**, *20*, 100468. [CrossRef]
84. Guo, X.; Zhang, G.; Wu, C.; Liu, J.; Li, G.; Zhao, Y.; Wang, Y.; Xu, Y. A cost-effective synthesis of heteroatom-doped porous carbon by sulfur-containing waste liquid treatment: As a promising adsorbent for CO_2 capture. *J. Environ. Chem. Eng.* **2021**, *9*, 105165. [CrossRef]
85. Park, J.; Cho, S.Y.; Jung, M.; Lee, K.; Nah, Y.-C.; Attia, N.F.; Oh, H. Efficient synthetic approach for nanoporous adsorbents capable of pre-and post-combustion CO_2 capture and selective gas separation. *J. CO_2 Util.* **2021**, *45*, 101404. [CrossRef]
86. Thommes, M.; Kaneko, K.; Neimark, A.V.; Olivier, J.P.; Rodriguez-Reinoso, F.; Rouquerol, J.; Sing, K.S. Physisorption of gases, with special reference to the evaluation of surface area and pore size distribution (IUPAC Technical Report). *Pure Appl. Chem.* **2015**, *87*, 1051–1069. [CrossRef]
87. Chuah, C.Y.; Lee, Y.; Bae, T.-H. Potential of adsorbents and membranes for SF_6 capture and recovery: A review. *Chem. Eng. J.* **2021**, *404*, 126577. [CrossRef]
88. Mason, J.A.; McDonald, T.M.; Bae, T.-H.; Bachman, J.E.; Sumida, K.; Dutton, J.J.; Kaye, S.S.; Long, J.R. Application of a high-throughput analyzer in evaluating solid adsorbents for post-combustion carbon capture via multicomponent adsorption of CO_2, N_2, and H_2O. *J. Am. Chem. Soc.* **2015**, *137*, 4787–4803. [CrossRef]
89. Myers, A.L.; Prausnitz, J.M. Thermodynamics of mixed-gas adsorption. *AIChE J.* **1965**, *11*, 121–127. [CrossRef]
90. Li, W.; Chuah, C.Y.; Yang, Y.; Bae, T.-H. Nanocomposites formed by in situ growth of NiDOBDC nanoparticles on graphene oxide sheets for enhanced CO_2 and H_2 storage. *Micropor. Mesopor. Mater.* **2018**, *265*, 35–42. [CrossRef]
91. Serre, C.; Bourrelly, S.; Vimont, A.; Ramsahye, N.A.; Maurin, G.; Llewellyn, P.L.; Daturi, M.; Filinchuk, Y.; Leynaud, O.; Barnes, P. An explanation for the very large breathing effect of a metal–organic framework during CO_2 adsorption. *Adv. Mater.* **2007**, *19*, 2246–2251. [CrossRef]
92. Lin, R.-B.; Li, L.; Wu, H.; Arman, H.; Li, B.; Lin, R.-G.; Zhou, W.; Chen, B. Optimized separation of acetylene from carbon dioxide and ethylene in a microporous material. *J. Am. Chem. Soc.* **2017**, *139*, 8022–8028. [CrossRef]
93. Lee, J.; Chuah, C.Y.; Kim, J.; Kim, Y.; Ko, N.; Seo, Y.; Kim, K.; Bae, T.H.; Lee, E. Separation of acetylene from carbon dioxide and ethylene by a water-stable microporous metal–organic framework with aligned imidazolium groups inside the channels. *Angew. Chem. Int. Ed.* **2018**, *130*, 7995–7999. [CrossRef]
94. Chuah, C.Y.; Goh, K.; Bae, T.-H. Hierarchically structured HKUST-1 nanocrystals for enhanced SF_6 capture and recovery. *J. Phys. Chem. C* **2017**, *121*, 6748–6755. [CrossRef]
95. Chuah, C.Y.; Yang, Y.; Bae, T.-H. Hierarchically porous polymers containing triphenylamine for enhanced SF6 separation. *Micropor. Mesopor. Mater.* **2018**, *272*, 232–240. [CrossRef]
96. Chuah, C.Y.; Yu, S.; Na, K.; Bae, T.-H. Enhanced SF_6 recovery by hierarchically structured MFI zeolite. *J. Ind. Eng. Chem.* **2018**, *62*, 64–71. [CrossRef]
97. Bae, Y.S.; Snurr, R.Q. Development and evaluation of porous materials for carbon dioxide separation and capture. *Angew. Chem. Int. Ed.* **2011**, *50*, 11586–11596. [CrossRef]
98. Bae, T.-H.; Hudson, M.R.; Mason, J.A.; Queen, W.L.; Dutton, J.J.; Sumida, K.; Micklash, K.J.; Kaye, S.S.; Brown, C.M.; Long, J.R. Evaluation of cation-exchanged zeolite adsorbents for post-combustion carbon dioxide capture. *Energy Environ. Sci.* **2013**, *6*, 128–138. [CrossRef]
99. Jiang, L.; Gonzalez-Diaz, A.; Ling-Chin, J.; Roskilly, A.; Smallbone, A. Post-combustion CO_2 capture from a natural gas combined cycle power plant using activated carbon adsorption. *Appl. Energy* **2019**, *245*, 1–15. [CrossRef]
100. Yang, W.-C.; Hoffman, J. Exploratory design study on reactor configurations for carbon dioxide capture from conventional power plants employing regenerable solid sorbents. *Ind. Eng. Chem. Res.* **2009**, *48*, 341–351. [CrossRef]
101. Majchrzak-Kucęba, I.; Wawrzyńczak, D.; Ściubidło, A.; Zdeb, J.; Smółka, W.; Zajchowski, A. Stability and regenerability of acivated carbon used for CO_2 removal in pilot DR-VPSA unit in real power plant conditions. *J. CO_2 Util.* **2019**, *29*, 1–11. [CrossRef]
102. Wawrzyńczak, D.; Majchrzak-Kucęba, I.; Srokosz, K.; Kozak, M.; Nowak, W.; Zdeb, J.; Smółka, W.; Zajchowski, A. The pilot dual-reflux vacuum pressure swing adsorption unit for CO_2 capture from flue gas. *Sep. Purif. Technol.* **2019**, *209*, 560–570. [CrossRef]